A Photoacoustic Sensing Probe Using Single Optical Fiber Acoustic Delay Line

Arif Kivanc Ustun, Student Member, IEEE, and Jun Zou, Senior Member, IEEE

Abstract—In this paper, we report a new photoacoustics (PA) sensing probe design using a single optical fiber for both light delivery and ultrasonic detection. This is made possible by the development and use of an optically transparent ultrasound transducer, which allows the excitation light to pass through and travel along the optical fiber to reach the target. In return, the transducer senses the generated PA signal transmitted through the optical fiber as an acoustic delay line. Optical transmission testing was performed to determine the transparency of the PMN-PT transducer. For demonstration, a prototype probe was designed, fabricated, and tested with black tape and red dye solutions as the target. The detection of an embedded target in the chicken breast was also demonstrated.

Index Terms—Photoacoustic sensing probes, biopsy needles, acoustic delay line, optical fiber, transparent transducer.

I. INTRODUCTION

OR biomedical applications, photoacoustics (PA) has become a useful technique that combines both rich optical absorption contrast and good acoustic penetration depth beyond optical diffraction limit [1], [2]. Although better than conventional optical methods, the penetration depth of PA sensing and imaging in tissues is still limited by the maximal allowable laser fluence and the optical absorption and acoustic attenuation in tissues [3]. In recent years, new PA sensing probe [4]-[6] or guided biopsy needles [7]-[9] have been developed to conduct localized measurements. Different from conventional optical sensing probes [10] (which could only consists of a single optical fiber for simultaneous light delivery and reception), the need for both light delivery and ultrasound detection poses some challenges in the design and construction of PA sensing probes, especially in terms of compactness. For in-vivo applications, the sensing probe needs to be as compact as possible to minimize its invasiveness.

To address this issue, we have demonstrated a new PA sensing probe design using two optical fibers [11]. One optical fiber serves as the optical waveguide for delivering excitation laser pulses onto the target. The second optical fiber functions as an acoustic delay line to detect and transmit the generated PA signals from the target to an outside ultrasound transducer, while creating a desirable amount of time delay. With the transducer located outside, the PA probe consists of only

Manuscript received May 2, 2019; accepted May 23, 2019. Date of publication June 6, 2019; date of current version September 5, 2019. This work was supported in part by an Award from NSF (ECCS # 1809710). The associate editor coordinating the review of this paper and approving it for publication was Dr. Daniele Tosi. (Corresponding authors: Arif Kivanc Ustun; Jun Zou.)

The authors are with the Department of Electrical and Computer Engineering, Texas A&M University, College Station, TX 77845 USA (e-mail: akustun87@tamu.edu; junzou@tamu.edu).

Digital Object Identifier 10.1109/JSEN.2019.2920931

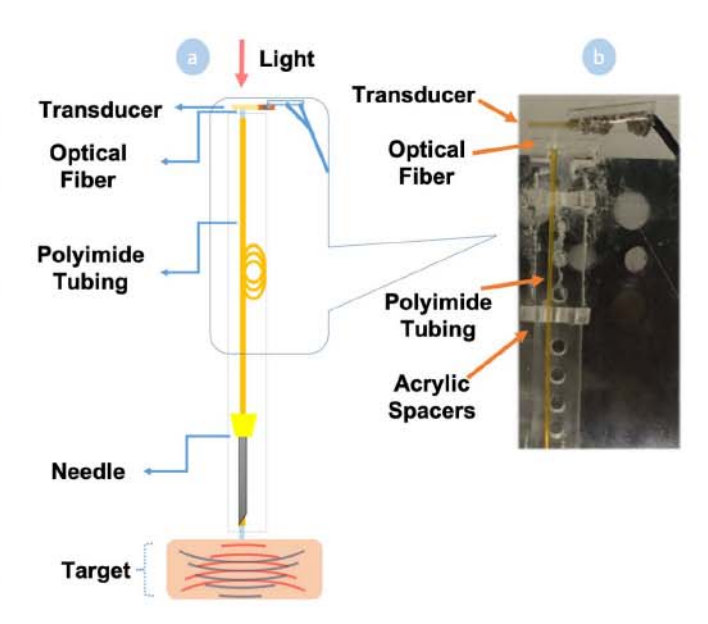


Fig. 1. a) Schematic of PA sensing probe design and b) picture of the constructed prototype.

two optical fibers placed closely to each other to provide a small probe diameter. In addition, by adding extra time delay, the PA signal will arrive at the transducer after all interference signals diminish and therefore can be easily distinguished and recorded for data processing. Still, with the use of two optical fibers, the PA sensing is not as compact as many optical sensing probes (with single optical fiber). In addition, the light delivery and the ultrasound detection areas are offset with each other, resulting in a non-ideal configuration for PA signal detection.

In this paper, we report a new PA sensing probe design using a single optical fiber for both light delivery and ultrasound detection. This is made possible by the development and use of an optically-transparent ultrasound transducer, which allows the excitation light to pass through and travel along the optical fiber to reach the target. In return, the transducer senses the generated PA signal transmitted through the optical fiber as an acoustic delay line. To make the optically-transparent ultrasound transducer, single-crystalline piezoelectric substrates and suitable electrode materials have been investigated. For demonstration, a prototype probe was designed, fabricated, and tested with different concentration of dye solutions and biological tissues with an embedded target.

II. PROBE DESIGN AND CONSTRUCTION

Fig. 1a shows the schematic design of the PA sensing probe. It consists of one single optical fiber laid out along

1558-1748 © 2019 IEEE. Personal use is permitted, but republication/redistribution requires IEEE permission. See http://www.ieee.org/publications_standards/publications/rights/index.html for more information.

the probe, which is housed inside a polyimide tubing. The polyimide tubing provides good structural protection and also acoustic insulation for the optical fiber [11]. During the operation of the probe, the optical fiber can easily contact with the surrounding tissue or medium. Without proper acoustic isolation, the transmitted PA signals can be completely damped out before reaching the transducer. The optical fiber serves a combined optical waveguide and acoustic delay line for sending laser pulses to the target and transmitting PA signal back from the target. To achieve this, the transducer is made optically transparent to avoid blocking the excitation light. A hollow needle can be used to provide better stability for the fiber tip of the probe. Fig. 1b shows the constructed prototype of the single optical fiber PA probe, which was securely positioned in a few acrylic spacers for stable measurements.

A. Optical Fiber Acoustic Delay Line

A single multimode optical fiber (FT400UMT, 0.39NA, Thorlabs, Newton, NJ) was used to make the optical fiber acoustic delay line. The polymer jacket layer of the acoustic delay fiber was removed to reduce the acoustic attenuation. The fiber core together with the cladding layer $(12.5-\mu m)$ thick) was placed inside a polyimide tubing (Microlumen, Oldsmar, FL) with an inner diameter (0.53 mm) slightly larger than that of the acoustic delay fiber. The polyimide tubing provides good structural protection and also acoustic insulation for the acoustic delay fiber. Without this isolation, the transmitted photoacoustic signals can be easily damped out by surrounding media. The diameter of the polyimide tubing does not significantly affect the PA response, as long as the optical fiber is loosely fitted inside the tubing. Therefore, a polyimide tube with an inner diameter slightly larger than the outer diameter of the optical fiber was used.

With a core diameter of 400 μ m, the multimode optical fiber provides a good balance of both optical and acoustic performances [12]. First, it can transmit 10s of µJ level nanosecond laser pulses without burning the tips. Second, the non-dispersive single-mode transmission frequency limit of the optical fiber is around $0.1 \sim 0.2 \ c/d$, where c and d are the acoustic velocity and the core diameter, respectively [13]. Suppose the acoustic velocity of the fiber core is \sim 5500 m/sec, this gives 1.25 \sim 2.5 MHz for a core diameter of 400 µm, which covers the peak frequency components of PA signals generated under unfocused illumination conditions. At $1\sim2$ MHz, the acoustic attenuation of the $400-\mu m$ fused silica core is very low, especially after the jacket layer is removed [11]. Therefore, the length of the optical fiber (and also the probe) can be determined mainly based on the need of the actual applications, as long as it is long enough to provide sufficient acoustic time delay to separate the real PA signal from interference caused by the firing of the pulsed laser.

Two-port ultrasound transmission test was performed to characterize the acoustic properties of the optical fiber (with jacket layer removed and placed inside the polyimide tubing). Two 2.25 MHz flat contact transducers were used to transmit and receive the ultrasound signals (Fig. 2a). The two ends of the acoustic delay fiber were polished and contacted onto the transmitting and receiving transducers, respectively. Mineral

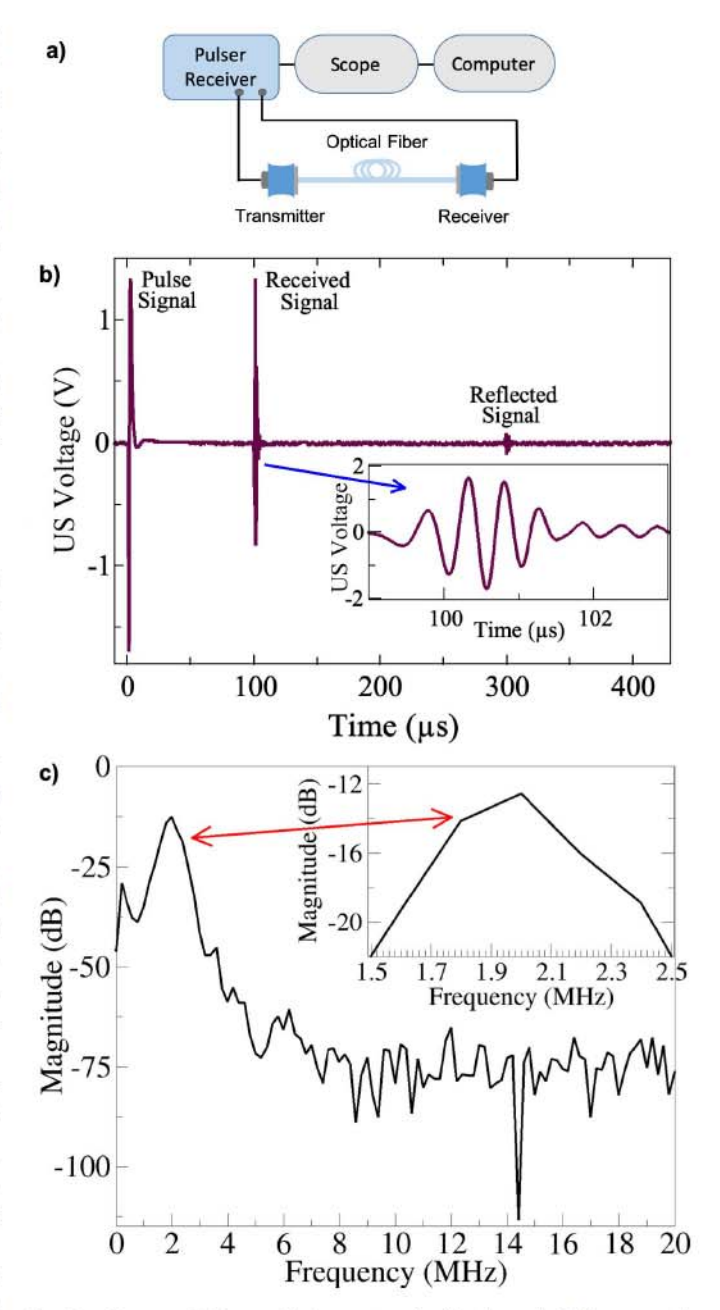


Fig. 2. Two port US transmission test results for the optical fiber acoustic delay line with no jacket layer a) testing setup b) pulse, received and reflected signals c) frequency spectrum of the received signal through the optical fiber acoustic delay line.

oil was applied onto the contacts between the ends of the optical fiber and the surfaces of transmitting & receiving transducers to enhance coupling efficiency and minimize unwanted reverberation. Each received ultrasound signal was averaged 16 times and recorded on a digital oscilloscope. Fig. 2b shows the ultrasound transmission of the optical fiber with a length of 54 mm. The received ultrasound signal is located at $\sim 99~\mu s$, which is close to the calculated time delay based on the acoustic velocity of the fused silica [13], [14]. Fig. 2c shows the frequency spectra of the transmitted ultrasound signal. The received (time-domain) ultrasound signal is truncated to remove the unwanted reverberations (i.e., the long tail). In other words, only significant time-domain information of

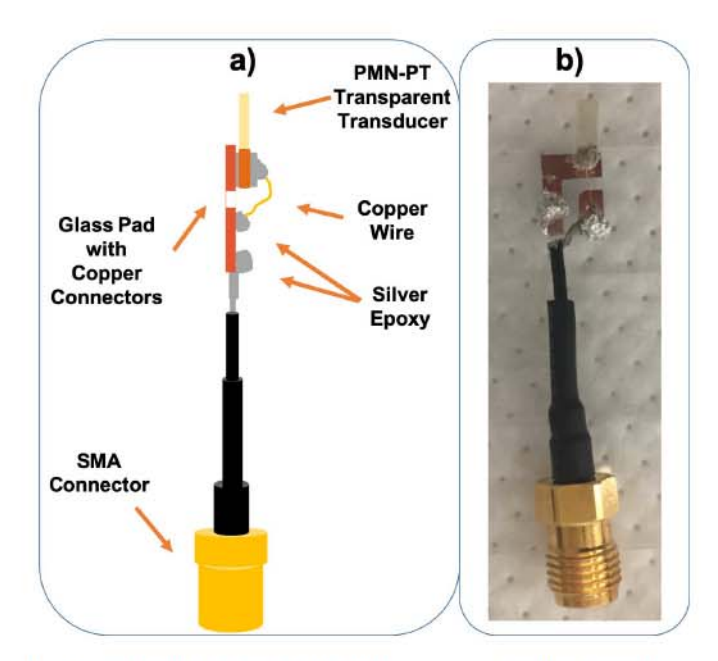


Fig. 3. Optically transparent PMN-PT transducer assembly in a) side view illustration and b) photo of the assembly.

the received ultrasound signal is selected. FFT (Fast-Fourier Transform) was performed in Matlab® to calculate the frequency spectra. The central frequency of the received signal is clearly seen at 2 MHz, matching the lowest longitudinal-mode transmission signals through the optical fiber [13].

B. Transparent Transducer

A piece of single crystalline PMN-PT (Pb(Mg_{1/3}Nb_{2/3})-PbTiO₃) substrate (HC Materials Corporation, Bolingbrook, Illinois, USA) was used to make the transparent transducer due to its good optical transparency and piezoelectric property. It has 27-33% PT content that varies the piezoelectric constant from 2000 pC/N and 3000 pC/N with <001> poling [15], [16]. The thickness of the PMN-PT substrate was 0.6 mm, which provides a resonance frequency of \sim 3.5 MHz in the thickness mode [15], which is high enough to cover the center frequency of the optical fiber (2 MHz) and its effective bandwidth. The surface area (\sim 5 mm \times 2 mm) of the PMN-PT transducer was kept small to reduce the parasitic capacitance to the transducer. No matching layer was added between the PMN-PT transducer and the optical fiber because their acoustic impedance is close to each other. Both top and bottom surfaces of the PMN-PT substrate were first polished to reduce the surface roughness. To form the transparent electrodes, a 120-nm thick ITO (indium-tin oxide) layer was coated on both surfaces by sputtering which provides both sufficient optical transparency and good electrical conductivity [5]. To facilitate the wiring, two chromium and copper contact pads (one on the top and one on the bottom) were directly formed by evaporation through a shadow mask. After the deposition is complete, the PMN-PT transducer was mounted onto a glass holder. For the connection between the transducer and the glass pad, silver epoxy (Von Roll 3022 E-Solder®, Conductive Adhesive, Schenectady, NY, USA) was applied and cured. Transducer mounting was completed by attaching an SMA connector to the glass-transducer assembly (Fig.3).

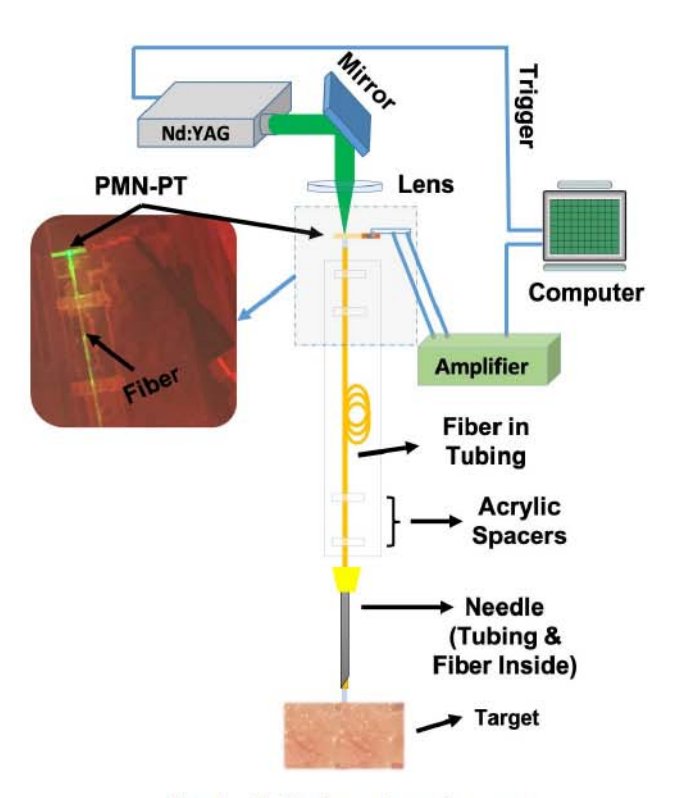


Fig. 4. PA Sensing probe testing setup.

III. TESTING AND CHARACTERIZATION

A. PA Testing Setup

The testing setup of the PA sensing probe is shown in Fig. 4. The light source was an Nd:YAG laser (SPOT-10-200-532, Elforlight Ltd, Northants, UK) operating at the wavelength of 532nm. Its pulse duration and maximum output energy were 1.75 ns and 20 μ J/pulse, respectively. The pulse repetition rate was set to 1 kHz. The output beam diameter was roughly 0.7 mm. A convex lens was used to focus the light onto the transparent transducer at a specific point. The optical fiber was aligned to the focal point of the light to provide maximal coupling efficiency. Multiple acrylic spacers and polyimide tubing were used to fix the optical fiber in a stable position. The focused light transmitted through the transparent transducer and the optical fiber, and then reached the target, which is made of a black vinyl electrical tape (Scotch® Super 33+ Vinyl Electrical Tape, USA). The black vinyl electrical tape has a high optical absorption coefficient and therefore provides high efficiency for PA signal generation. The contact conditions between the fiber tip and the transducer and target were carefully maintained during tests to reduce acoustic coupling loss between the optical fiber and the target or between the transducer and optical fiber. A home-made PCB amplifier was used to amplify the acoustic signal coming from the transparent transducer. Its amplitude gain was set to be 23 dB based on the values of feedback resistor and input resistor in an inverting amplifier [17]. The amplified PA signal is received by a digital oscilloscope with a sampling rate of 100 MHz.

B. Probe Characterization

After necessary alignments were made, the overall optical transmission efficiency through the transparent transducer was

TABLE I
OPTICAL TRANSMISSION EFFICIENCY MEASUREMENTS FOR
DIFFERENT TRANSDUCER SAMPLES

Material	Thickness	Transmission Efficiency (%)
Unpolished PMN-PT	1.6mm	~2 %
Unpolished PMN-PT	0.6mm	~11 %
Polished PMN-PT with ITO	1.6mm	~9 %
Polished PMN-PT with ITO	0.6mm	~25 %

first characterized. The target was replaced with the photodetector of an optical power meter. As a reference measurement, the transducer was first removed from the measurement setup and the optical power at the end of the fiber was measured by the power meter. The transducer substrate was put back and the optical power was measured again. The output laser power measured at the tip of PA sensing probe with and without the transparent transducer was 1.464 mW and 5.88 mW, respectively, which corresponds to an overall optical transmission efficiency of 24.9%. For comparison, an un-polished and also a thicker PMN-PT substrate was also measured to evaluate the transmission loss due to surface scattering and optical absorption inside PMN-PT (Table.1). As listed in Table.1, both thickness and surface condition of the PMN-PT substrate play a significant role in the optical transmission efficiency. To avoid excessive attenuation due to absorption, the thickness of the PMN-PT substrate needs to be carefully chosen to satisfy the requirements on both optical and acoustic performances. In addition, the surface roughness should be minimized to reduce the light loss due to scattering. Moreover, both PMN-PT and ITO have excellent transparency in the visible and near-infrared range. Since the optical transparency of PMN-PT and ITO have been well studied before [18]-[20], the optical transparency for the transducer quantified at single wavelength.

Fig. 5a shows a representative PA signal received from the black tape target after being averaged by sixteen times. In addition to the original PA signal (which arrived first), the second, third, and fourth reflected signals were also received at later times. This shows that the optical fiber can serve as a low-loss acoustic delay line to transmit the PA signal from the target to the transducer. Fig. 5b shows the FFT spectrum of the received PA signal. It covers a wide frequency range up to 2.1MHz, which corresponds to the cut-off frequency of the lowest longitudinal mode of the optical fiber.

For probe characterization, different laser power levels were used to reveal the relationship between the optical fluence and the resulting PA signal strength (Fig. 6). The laser pulse energy and the optical fluence were determined based on the measured laser power, the pulse repetition rate, and also the estimated illumination area. At the probe tip, the maximal pulse energy was $5.36~\mu\text{J/pulse}$ and the maximal optical fluence was $4.27~\text{mJ/cm}^2$, which is far below the ANSI (American National Standard Institute) safety limit of $20~\text{mJ/cm}^2$ [21]. As shown in Fig. 6, the PA voltage increase with the optical fluence with strong linear correlation ($R^2 = 0.991$).

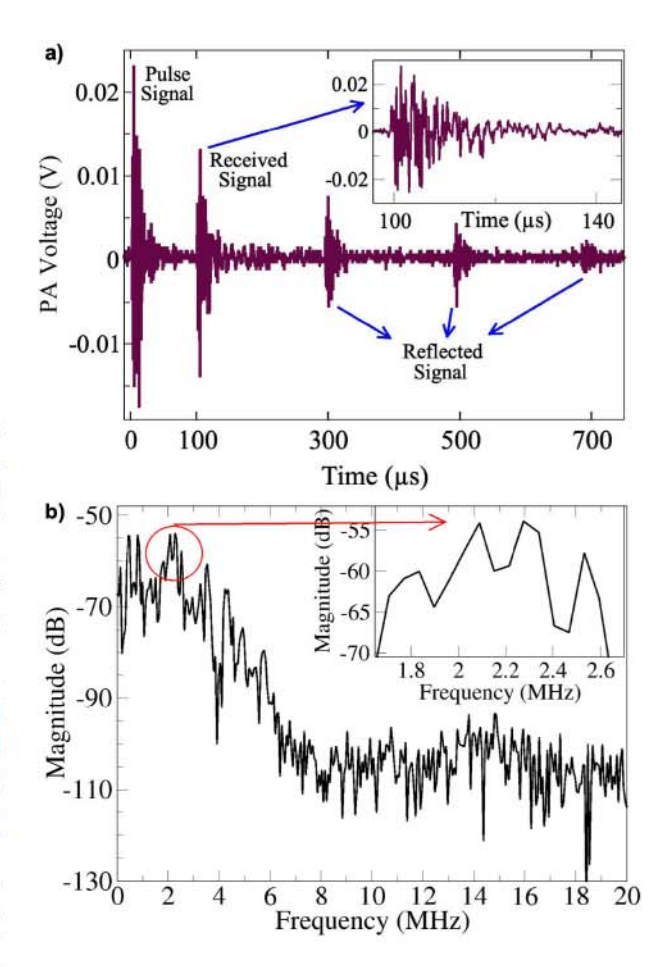


Fig. 5. PA test results of the PA sensing probe with black tape as the target a) pulse, received, and reflected signals b) frequency spectrum of the received PA signal.

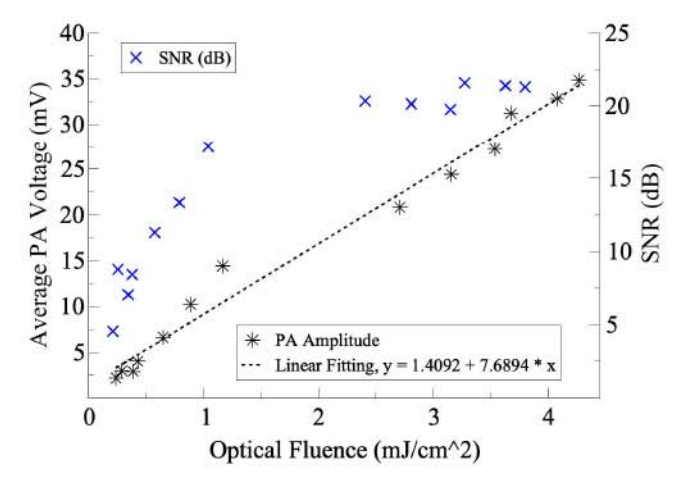


Fig. 6. PA voltage and SNR vs. optical fluence.

With an almost constant noise floor, the SNR increases with optical fluence by following a logarithmic relationship.

C. Dye Characterization

The PA testing setup was also used to demonstrate the PA characterization of dye concentration. The dye concentration testing is a common procedure to evaluate the sensitivity and linearity of a PA sensing or imaging system.

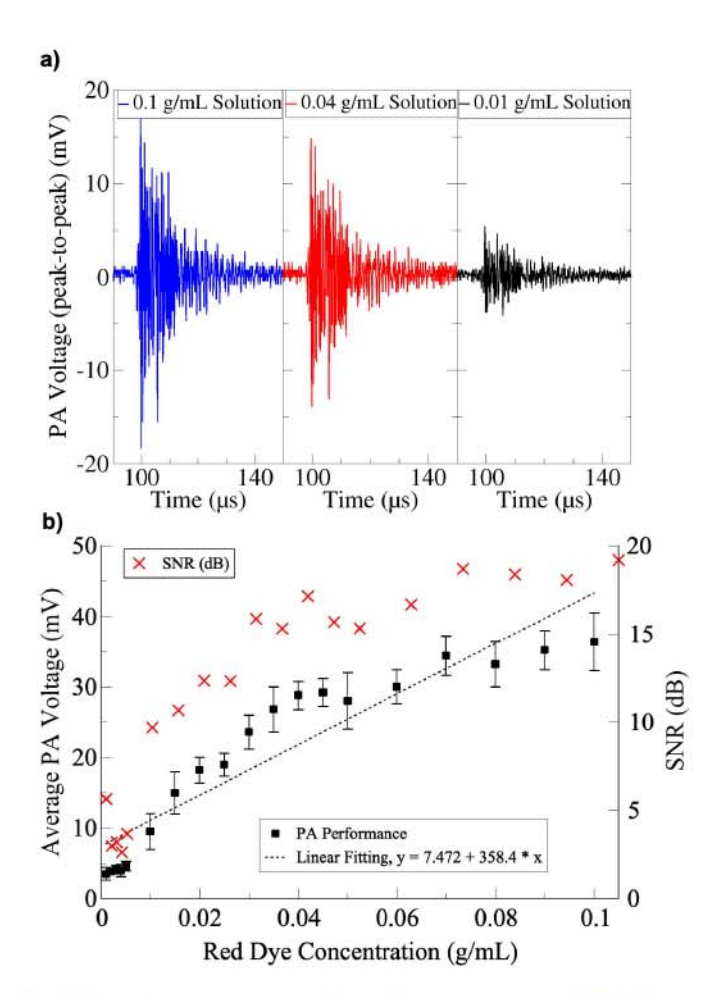


Fig. 7. a) PA signals received from Red Dye solutions with different concentrations: (Left) 0.1 g/mL, (Middle) 0.04 g/mL, and (Right) 0.01 g/mL. b) PA voltage and SNR vs. Dye concentration.

When a single die is used, the absorbed optical energy and the resulting PA response (i.e., the first peak of the PA signal from the transducer) should increase linearly with the dye concentration. By measuring the PA signals from dye solutions with different concentrations, the linearity of the PA sensing probe can be characterized. In addition, the lowest detectable dye concentration can serve as a good indication of the sensitivity. Dye solutions were prepared with red dye powders (Rit® Dye, Phoenix Brands, Stamford, CT). Powders were first dissolved in DI water and was transferred into an acrylic container. The PA sensing probe was first mounted onto a Z-stage and gradually lowered till the tip of the optical fiber just touched the surface of the dye solution. For each concentration, the PA measurement is repeated five times. The captured PA voltages were averaged to determine the overall PA response.

Fig. 7a shows the PA signals received from 0.1 g/mL, 0.04 g/mL, and 0.01 g/mL red dye solutions. The change in the average PA voltage of the first peaks as a function of the red dye concentration from 0.001 g/mL to 0.1 g/mL is shown in Fig. 7b. The peak PA voltage increases with the dye concentration, showing a significant linear correlation between the dye concentration and the PA response of the probe ($R^2 = 0.928$). When the dye concentration was reduced

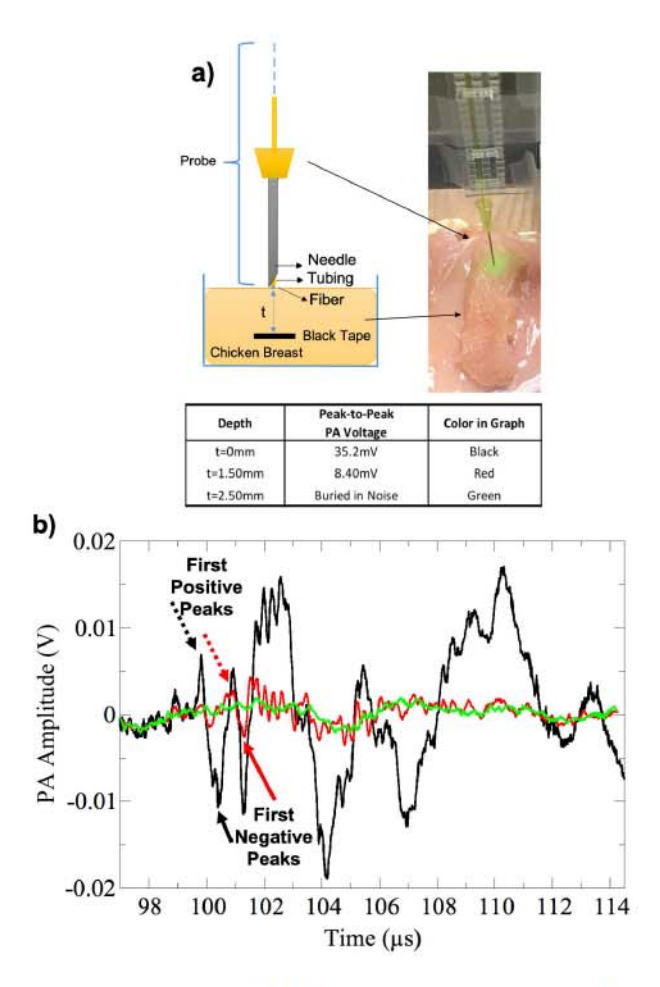


Fig. 8. PA ex-vivo tests with chicken breast a) testing setup and b) PA signals from different depths.

down from 0.1 g/mL to 0.001 g/mL, SNR dropped from 19.2dB to 5.63dB. The received PA waveform started to bury under the noise level, which indicates a detection limit of about 0.001 g/mL.

D. Target Depth Detection in Biological Tissues

Detecting targets at different depths in biological tissues is another important function of the PA sensing probe. The PA measurements at different depths were performed in chicken breast to mimic ex-vivo testing in biological tissues. As shown in Fig. 8a, a piece of black tape was placed underneath the chicken breast to serve as the target. The PA sensing probe was placed onto a piece of chicken breast, with its tip gently touching the surface of the chicken breast. Fig. 8b shows the received PA signals at three different depths (t) of 0 mm (black), 1.50 mm (red), and 2.50 mm (green), respectively.

Upon excitation of laser pulses, the PA signal from the black-tape target travels through the chicken breast tissue and the optical fiber, and reaches the transducer after certain amount of time. The first positive or negative peak of the recorded PA voltage represents the original PA response. After impinging on the transducer, the PA signal could induce some secondary resonant responses on the transducer, which manifest themselves as lower-frequency oscillations at later times. The PA signal amplitude dropped when the thickness

of the chicken breast increased, which is mainly due to lower optical fluence caused by stronger light diffusion at larger depth. At t = 2.5 mm, the PA signal started to be buried into noise, indicating the maximal detection depth under the current testing condition. Based on the chicken breast's acoustic velocity, the depth of the target was estimated from the time delay difference between the corresponding positive or negative peaks of the PA signals between the two measurements (0 mm (red) and 1.5 mm (black)). As shown in Fig. 8b, the delay time difference of the two first positive and negative peaks of the PA signals from the target at 0 mm and 1.5mm is 1.2 μ s and 0.96 μ s, respectively. Assuming the acoustic velocity of the chicken breast is 1540 m/s, the estimated depth is 1.77 mm and 1.48mm, respectively, which match the actual depth (1.5 mm) of the black tape target.

IV. CONCLUSIONS

In this paper, a new PA sensing probe design using a single optical fiber acoustic delay line and an optically-transparent PMN-PT transducer has been demonstrated. By using a single optical fiber for both light delivery and ultrasound reception, a compact and minimally-invasive probe structure can be achieved. Capitalizing upon the optical transparency of the PMN-PT substrate, the transducer can be placed between the optical source and the optical fiber, allowing the light delivery and transmission of the acoustic signals through the same optical fiber. As a result, the light delivery and the ultrasound detection are automatically aligned with each other, thereby resulting in an optimal configuration for PA signal detection. Although the initial concept has been demonstrated, several improvements will need to be investigated in future work. First, the optical transmission efficiency can be improved by optimizing the contacts and refractive index matching between the PMN-PT substrate and optical fiber. Second, an acoustic impedance matching layer can be added onto the optical fiber to improve the efficiency of PA signal collection. Third, a bundle of smaller optical fibers can be used to transmit higher frequency components of the PA signal to enhance the depth resolution of PA detection.

REFERENCES

- [1] A. Oraevsky and A. Karabutov, "Optoacoustic tomography," in Biomedical Photonics Handbook, vol. 34. Boca Raton, FL, USA: CRC Press, 2003, pp. 1-34.
- [2] L. V. Wang, Photoacoustic Imaging and Spectroscopy. Boca Raton, FL, USA: CRC Press, 2009.
- [3] J. Yao and L. V. Wang, "Sensitivity of photoacoustic microscopy," Photoacoustics, vol. 2, no. 2, pp. 87-101, Jun. 2014.
- [4] C. Kim, T. N. Erpelding, L. Jankovic, and L. V. Wang, "Performance benchmarks of an array-based hand-held photoacoustic probe adapted from a clinical ultrasound system for non-invasive sentinel lymph node imaging," Philos. Trans. Roy. Soc. A, Math. Phys. Sci., vol. 369, no. 1955, pp. 4644-4650, Nov. 2011.
- [5] W. Xia et al., "Fiber optic photoacoustic probe with ultrasonic tracking for guiding minimally invasive procedures," in Proc. Eur. Conf. Biomed. Opt., Jan. 2015, Art. no. 95390K.

- [6] Y. Cho et al., "Handheld photoacoustic tomography probe built using optical-fiber parallel acoustic delay lines," J. Biomed. Opt., vol. 19, no. 8, 2014, Art. no. 086007.
- [7] D. Piras, C. Grijsen, P. Schütte, W. Steenbergen, and S. Manohar, "Photoacoustic needle: Minimally invasive guidance to biopsy," J. Biomed. Opt., vol. 18, no. 7, Jul. 2013, Art. no. 070502.
- [8] G. Xu et al., "Photoacoustic biopsy: A feasibility study," Proc. SPIE, vol. 9318, Mar. 2015, Art. no. 931806.
- [9] P. M. Phal, D. M. Brooks, and R. Wolfe, "Sonographically guided biopsy of focal lesions: A comparison of freehand and probe-guided techniques using a phantom," Amer. J. Roentgenol., vol. 184, no. 5, pp. 1652-1656, May 2005.
- [10] R. J. Colchester et al., "Real-time needle guidance with photoacoustic and laser-generated ultrasound probes," Proc. SPIE, vol. 9323, Mar. 2015, Art. no. 932321.
- [11] A. K. Ustun and J. Zou, "A photoacoustic sensing probe using optical
- fiber acoustic delay line," *Photoacoustics*, vol. 13, pp. 18–24, Mar. 2019. [12] M. K. Yapici *et al.*, "Parallel acoustic delay lines for photoacoustic tomography," J. Biomed. Opt., vol. 17, no. 11, Nov. 2012, Art. no. 116019.
- [13] I. L. Gelles, "Optical-fiber ultrasonic delay lines," J. Acoust. Soc. Amer., vol. 39, no. 6, pp. 1111-1119, Jun. 1966.
- [14] G. D. Boyd, L. A. Coldren, and R. N. Thurston, "Acoustic clad fiber delay lines," IEEE Trans. Sonics Ultrason., vol. 24, no. 4, pp. 246-252, Jul. 1977.
- [15] K. C. Cheng, H. L. W. Chan, C. L. Choy, Q. R. Yin, H. S. Lu, and Z. W. Yin, "Piezoelectric coefficients of PMN-0.33PT single crystals," in Proc. 12th IEEE Int. Symp. Appl. Ferroelectr., vol. 2, Jul. 2000, pp. 533-536.
- [16] H. J. Lee, S. Zhang, J. Luo, F. Li, and T. R. Shrout, "Thicknessdependent properties of relaxor-PbTiO3 ferroelectrics for ultrasonic transducers," Adv. Funct. Mater., vol. 20, no. 18, pp. 3154-3162,
- [17] C. Fang, A. Ustun, Y. Cho, and J. Zou, "A charge amplification approach for photoacoustic tomography (PAT) with parallel acoustic delay line (PADL) arrays," Meas. Sci. Technol., vol. 28, no. 5, Mar. 2017, Art. no. 055108.
- [18] H. Jiang et al., "Transparent electro-optic ceramics and devices," Proc. SPIE, vol. 5644, pp. 380-395, Jan. 2005.
- [19] M. D. E. M. Benoy, M. S. Babu, P. J. Binu, and B. Pradeep, "Thickness dependence of the properties of indium tin oxide (ITO) FILMS prepared by activated reactive evaporation," Brazilian J. Phys., vol. 39, no. 4, Dec. 2009.
- [20] X. Wan, H. Luo, and X. Z. A. Zhao, "Feasibility of growing and optical properties of ferroelectric," in *Trends in Crystal Growth Research*. New York, NY, USA: Nova Publishers, 2005, p. 45.
- American National Standard for the Safe Use of Lasers, Standards ANSIZ136, ANSftSUo, American National Standards Institute, New York, NY, USA, 2007.

Arif Kivanc Ustun was born in Mugla, Turkey. He received the B.Sc. degree from Anadolu University, Eskisehir, Turkey, in 2009, and the M.Eng. degree from Texas A&M University in 2014, where he is currently pursuing the Ph.D.

His current research interests include microelectromechanical systems (MEMS), acoustic/ultrasonic delay lines, novel photoacoustic/ultrasonic medical systems, and related micro-nano fabrication methods.

Jun Zou (SM'98-M'04-SM'15) received the Ph.D. degree in electrical engineering from the University of Illinois at Urbana-Champaign in 2002.

In 2004, he joined the Department of Electrical and Computer Engineering, Texas A&M University, where he is currently a Full Professor. His current research interests lie in the development of micro- and nano-opto-electromechanical devices and systems for biomedical imaging and sensing applications. He is a Senior Member of SPIE and a member of OSA.